

Switching the Mechanism of NADH Photooxidation by Supramolecular Interactions

Alexander K. Mengele,^[a] Dominik Weixler,^[b] Avinash Chettri,^[c, d] Maite Maurer,^[a] Fabian Lukas Huber,^[a] Gerd M. Seibold,^[b, e] Benjamin Dietzek,^[c, d] Bernhard J. Eikmanns,^[b] and Sven Rau^{*[a]}

Abstract: A series of three Ru(II) polypyridine complexes was investigated for the selective photocatalytic oxidation of NAD(P)H to NAD(P)⁺ in water. A combination of (time-resolved) spectroscopic studies and photocatalysis experiments revealed that ligand design can be used to control the mechanism of the photooxidation: For prototypical Ru(II) complexes a ¹O₂ pathway was found. **Rudppz** ([[(tbbpy)₂Ru(dppz)]Cl₂, tbbpy = 4,4'-di-*tert*-butyl-2,2'-bipyridine, dppz = dipyrido[3,2-*a*:2',3'-*c*]phenazine), instead, initiated the cofactor oxidation by electron transfer from NAD(P)H enabled by supramolecular binding between substrate and catalyst. Expulsion of the photoproduct NAD(P)⁺ from the supramolecular binding site in **Rudppz** allowed very efficient turnover. Therefore, **Rudppz** permits repetitive selective assembly and oxidative conversion of reduced naturally occurring nicotinamides by recognizing the redox state of the cofactor under formation of H₂O₂ as additional product. This photocatalytic process can fuel discontinuous photobiocatalysis.

Due to their impressive catalytic activity and high stereoselectivity under ambient aqueous conditions, enzymatic oxidation reactions are recently gaining significant relevance even on an industrial level.^[1] Typically, O₂ or NAD⁺ (oxidized nicotinamide adenine dinucleotide) are used as oxidants.^[1,2] Due to the high costs of the important cofactor NAD⁺, a variety of enzyme-based^[2,3] as well as chemical^[4,5] and

electrochemical^[6,7] regeneration methods have already been developed.

In order to also exploit the energy of visible light for NAD⁺ regeneration, processes based on either organic dyes,^[8,9] photosensitive polymers^[10] or inorganic dyes such as tin porphyrines,^[11] Ru(II),^[12,13] Os(II),^[14] and Ir(III)^[15,16] complexes have been developed. Additionally, NADH photooxidation has recently also been successfully investigated as a mode of action in photodynamic therapy (PDT).^[14–17] In all these light-driven processes, NADH oxidation is either induced via formation of ¹O₂^[18–20] by the excited chromophore or by electron transfer (eT) onto the excited^[8,9,11,15] or photooxidized^[12,13,16] dye.

A specific subclass of Ru(II) complexes, those bearing large planar ligands, is known to interact with nucleobases inside the DNA.^[21–24] As NAD(P)H contains an adenine subunit, we thus wondered whether such preorganization might lead to improved light-driven cofactor oxidation stimulated by supramolecular interactions. To test this hypothesis, a simple series of three prototype chromophores, namely [Ru(tbbpy)₃]Cl₂ (**Rutbbpy**), [(tbbpy)₂Ru(phen)]Cl₂ (**Ruphen**) and [(tbbpy)₂Ru(dppz)]Cl₂ (**Rudppz**) was investigated with respect to their photooxidative properties (Scheme 1, tbbpy = 4,4'-di-*tert*-butyl-2,2'-bipyridine, phen = 1,10-phenanthroline, dppz = dipyrido[3,2-*a*:2',3'-*c*] phenazine).

The water soluble complexes **Rutbbpy**, **Ruphen** and **Rudppz** were synthesized according to established protocols^[25] (see Supporting Information and Figures S1–S21). Their photooxidative activity towards NADH under ambient aqueous conditions was evaluated using LED-irradiation (λ_{max} = 465 nm) in presence of 500 equivalents NADH (see Supporting Informa-

[a] A. K. Mengele, M. Maurer, F. L. Huber, Prof. S. Rau
 Institute of Inorganic Chemistry I, Materials and Catalysis
 Ulm University
 Albert-Einstein-Allee 11, 89081 Ulm (Germany)
 E-mail: sven.rau@uni-ulm.de

[b] D. Weixler, Prof. G. M. Seibold, Prof. B. J. Eikmanns
 Institute of Microbiology and Biotechnology
 Ulm University
 Albert-Einstein-Allee 11, 89081 Ulm (Germany)

[c] A. Chettri, Prof. B. Dietzek
 Department Functional Interfaces
 Leibniz Institute of Photonic Technology Jena
 Albert-Einstein-Allee 9, 07745 Jena (Germany)

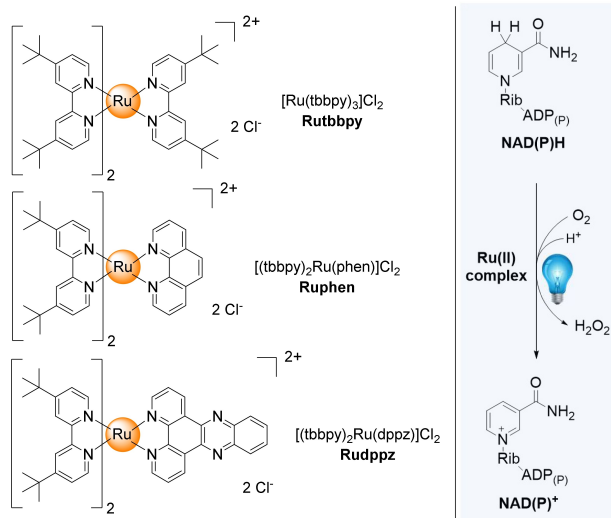
[d] A. Chettri, Prof. B. Dietzek
 Institute of Physical Chemistry
 Friedrich-Schiller University Jena
 Helmholtzweg 4, 07743 Jena (Germany)

[e] Prof. G. M. Seibold
 Section of Synthetic Biology
 Department of Biotechnology and Bioengineering
 Technical University of Denmark
 Søtoftsplads, 2800 Kongens Lyngby (Denmark)

Supporting information for this article is available on the WWW under <https://doi.org/10.1002/chem.202103029>

Part of a Special Issue on Contemporary Challenges in Catalysis.

© 2021 The Authors. Chemistry - A European Journal published by Wiley-VCH GmbH. This is an open access article under the terms of the Creative Commons Attribution Non-Commercial NoDerivs License, which permits use and distribution in any medium, provided the original work is properly cited, the use is non-commercial and no modifications or adaptations are made.



Scheme 1. Molecular structure and abbreviations of the complexes (left) and reaction scheme of the investigated Ru(II) complex catalyzed NAD(P)H photooxidation (right; Rib = β-D-ribofuranose, ADP(P) = (phosphorylated) adenosine diphosphate).

tion for experimental details). All three complexes proved to be active NADH photooxidation catalysts as indicated by the continuously decreasing 340 nm absorbance and 460 nm centered emission band (Figures 1A and B) both being characteristic for the reduced nicotinamide moiety.^[26] A nearly quantitative conversion of NADH to NAD⁺ under these conditions was obtained, if the samples were irradiated for 2 h (>99% for **Rutbbpy** and **Rudppz**, >95% for **Ruphen**, Figure S22). No spectral shifts indicative of products different to NAD⁺ (non-emissive if $\lambda_{\text{exc}} = 340$ nm, Figure S23) were observed.^[27] ¹H NMR spectroscopy also proved the selective formation of NAD(P)⁺ from NAD(P)H (Figures S24–S25). Despite its negligible ¹O₂ formation in H₂O containing solutions monitored by NIR emission spectroscopy (Figure S26),^[28] **Rudppz** exhibited the fastest NADH photooxidation in H₂O (initial TOF > 1000 h⁻¹) followed by **Ruphen** and **Rutbbpy** (Figure 1C).

To evaluate the mechanism of the oxidation reactions, a series of control experiments was performed. NADH oxidation was neither observed in the dark nor in the absence of oxygen or Ru(II) complex (Figure S27). No UV-vis or ¹H NMR spectroscopic changes were found, if NAD⁺ was irradiated in presence of a photocatalyst indicating that NAD⁺ represented the end-

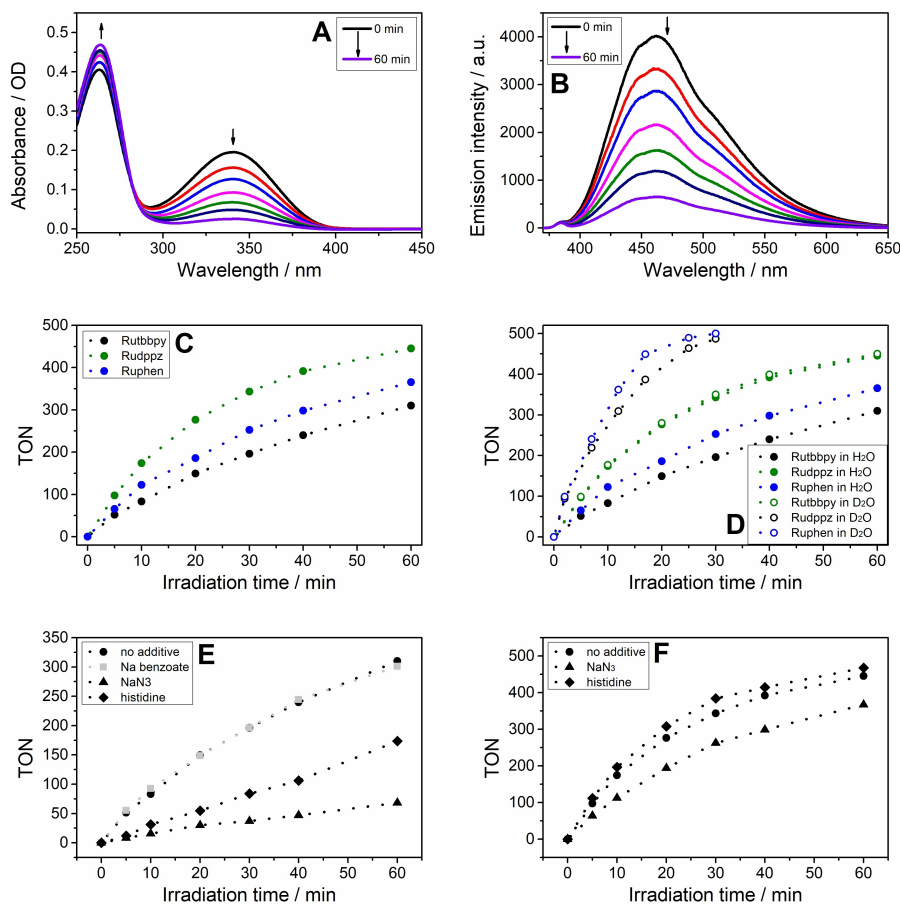


Figure 1. A) UV-vis and B) corresponding emission spectroscopic changes during the NADH photooxidation with **Rudppz** in H₂O. C) TON-plot for the three photocatalysts in H₂O (1 mM NADH, 2 μM photocatalyst). D) Effect of solvent deuteration on the NADH photooxidation rate. E) Effect of ROS quenchers on the NADH photooxidation rate using **Rutbbpy** or F) **Rudppz** as catalyst.

point of the reaction (Figures S27–S28). Furthermore, by adding 15 mM of the known OH radical scavenger sodium benzoate to the solution, the rate of NADH photooxidation choosing **Rutbbpy** as catalyst was not altered (Figure 1E). Thus, OH radicals as reactive oxygen species (ROS) were excluded to decisively contribute to the photooxidation.^[29]

However, both the addition of 15 mM NaN₃ or 15 mM histidine strongly reduced the NADH photooxidation rate using **Rutbbpy** and **Ruphen** (Figure 1E, Figure S29). Based on the additives' property to act as ¹O₂ quenchers,^[29–31] a reaction mechanism proceeding via ¹O₂ formation from the ³MLCT excited state of **Rutbbpy** or **Ruphen** initiating the oxidation of NADH was proposed. The ¹O₂ pathway for **Rutbbpy** and **Ruphen** was further supported by the fact that significant luminescence quenching for both complexes was only observed in presence of 250 μM oxygen but not 250 μM NADH (Figure S30) as well as the finding that changing the solvent from H₂O to D₂O led to an accelerated photooxidation (see Figure 1D) which we ascribe to the prolonged lifetime of ¹O₂ in D₂O.^[32] Thus, using D₂O and low concentrations of **Ruphen**, TONs up to 3600 after 3.5 h were realized (Figure S31).

Rudppz revealed a different behavior: The addition of neither NaN₃ nor histidine (Figure 1F) nor deuteration of the solvent (Figure 1D) impacted the NADH photooxidation rate considerably. Hence, we suggest an eT mechanism to be active.^[15] This is supported by monitoring the ¹O₂-driven photooxidation of histidine,^[31] proceeding for **Rudppz** drastically slower than for **Rutbbpy** and **Ruphen** (Figures S32–S33).

To take a closer look into the eT mechanism, transient absorption (TA) spectroscopy was performed (Figure 2). When **Rudppz** and NADH are mixed, the femtosecond (fs-)TA showed the formation of an excited state absorption centered at 490 nm (purple line, Figure 2A, Figures S34C and D) in both, absence and presence of oxygen. This band is likely associated to the oxygen-sensitive,^[33] phenazine-hydrogenated **Rudppz**_{H₂}, which is assumed to form immediately upon excitation of **Rudppz**. No **Rudppz**_{H₂} feature at 490 nm was observed in fs-TA of **Rudppz** without NADH (Figure S34A–B). For **Rudppz** mixed with NADH in the presence of oxygen, predominant signatures from NADH radicals (NADH^{•+}/NAD[•]) could only be observed in the nanosecond (ns-) TA and not in the fs-TA spectra (Figure 2).

This was due to the more dominant spectral signature of **Rudppz**_{H₂} in the fs range than the spectral signatures from the NADH radicals. Photoexcited **Rudppz**_{H₂} decays within a μs thereby showcasing the spectral signatures corresponding to NADH radicals, which typically have a much longer lifetime, only after this time delay (Figure S35).

ns-TA reveal accumulation of **Rudppz**_{H₂} (blue line, Figure 2B). During the experiment performed under inert conditions no features of NAD radicals could be recorded anymore (Figure S35). However, as upon exposure to air **Rudppz** was reformed (Figure 3B) and subsequently NAD radicals were detected in the ns-TA spectra again (black line, Figure 2A and Figure S35), **Rudppz** followed a similar eT based NADH photooxidation mechanism as reported for flavin dyes.^[8,9] To enter a new cycle, the photochemically reduced and inactivated chromophore **Rudppz**_{H₂} has to be reoxidized by oxygen. This ability of oxygen has already been shown.^[33]

To further verify the mechanistic differences between **Rutbbpy** and **Ruphen** vs. **Rudppz**, NADH photooxidation under exclusion of oxygen but in presence of H₂O₂ serving as oxidant for reduced chromophore species was performed. As NAD⁺ formation was only observed for **Rudppz** (Figures S36), **Rutbbpy** and **Ruphen** are strictly oxygen-dependent catalysts whereas **Rudppz** also operates in presence of a different oxidant. Stability of NADH even in presence of large excess H₂O₂ was verified (Figure S37).

The very surprising ability of **Rudppz** to outcompete the significantly longer-lived **Rutbbpy** and **Ruphen** in a photocatalytic redox reaction in H₂O^[37] was further investigated by ¹H NMR spectroscopy. Addition of NADH but not NAD⁺ led to significant mutual shifts of signals assigned to the terminal benzene ring of the dppz ligand and the adenine protons (Figure 3 and Figures S38–S41). The adenine-mediated interaction is furthermore supported by similar ¹H NMR spectroscopic shifts upon addition of structurally analogous ADP (Figures S42–S44). This further confirms, that NADH is preorganized at the dppz ligand of **Rudppz** via the nucleobase moiety, thus enabling efficient photooxidation of the cofactor due to close spatial proximity.^[15] No such interaction with NADH was observed for **Ruphen** (Figure S45–S46). Titration experiments resulted in binding constants of 30.7 ± 7.4 M⁻¹ for NADH and

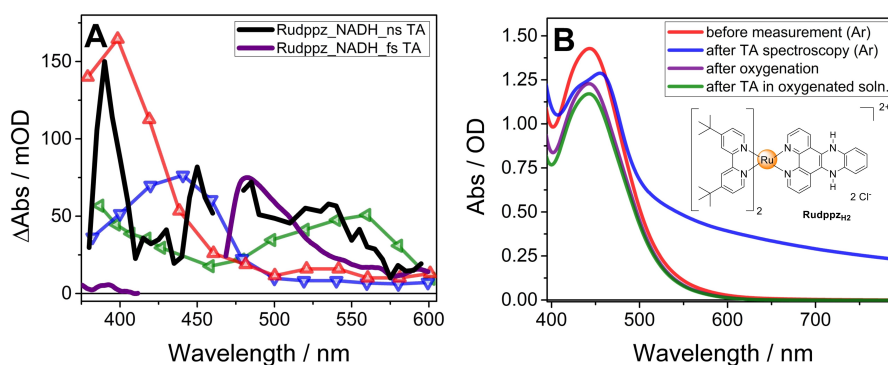


Figure 2. A) fs-TA and ns-TA spectra of the **Rudppz**/NADH system in the presence of oxygen at 470 nm excitation along with reference spectra for NADH^{•+} (red and green traces).^[34–36] B) Ground-state UV-vis absorption spectra of the system during the course of the ns-TA experiment.

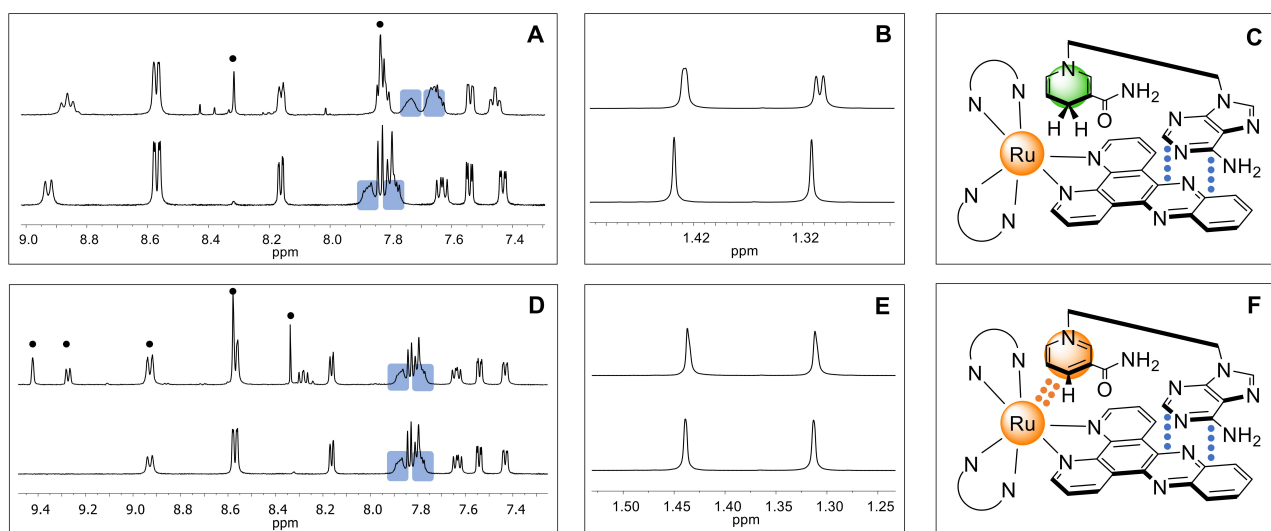


Figure 3. ^1H NMR spectroscopic shifts of 4 mM **Rudppz** (bottom spectrum in every NMR-panel, $\text{D}_2\text{O}:\text{d}_6\text{-DMSO} = 55:45$ (v:v)) upon addition of equimolar amounts of NADH (A, B) or NAD^+ (D, E; upper ^1H NMR spectra). C) and F) schematically indicate by colored dots the interactions between **Rudppz** and the reduced and oxidized nicotinamide, respectively (blue: attractive, orange: repulsive).

$23.5 \pm 4.3 \text{ M}^{-1}$ for ADP to **Rudppz** (Figures S42–S44 and S47–S48). Based on these rather low numbers, a dynamic exchange on the dppz sphere was verified by adding a 10-fold excess of ADP to a typical NADH photooxidation process. For **Rudppz** this resulted in an activity drop of only 12% (no change for **Ruphen**, Figure S49).

Together with the observed splitting of the aliphatic tbbpy resonances being larger for NADH than for ADP (Figures S44 and S48), a molecular picture of the above-mentioned oxidation-state sensitive interaction was delineated (Figures 3C and F): Upon photooxidation, the charge of the nicotinamide moiety is increased from neutral to onefold positive. Consequently the coulombic repulsion from the nearby Ru center, possibly in concert with other factors such as lowered lipophilicity,^[38] dominates over attractive π - π interactions.

Following the light induced O_2 consumption of the **Rudppz**/NADH system *in operando*^[39] in combination with associated UV-vis and emission spectroscopic data, a 1:1 stoichiometry between consumed oxygen and converted NADH was found (Figure 4, a \rightarrow b and Figure S50). Subsequent addition of catalase after all oxygen had been consumed (Figure 4A, step c), also allowed to determine a 1:1 ratio between the products H_2O_2 and NAD^+ , providing evidence that two high value products during the photocatalytic process were formed that could be used for further (biochemical) reactions.^[40]

Considering all results, a ligand-dependent switch of the NADH-photooxidation mechanism in the herein investigated series of photocatalysts is postulated (Scheme 2).^[18–20,41] **Rutbbpy** and **Ruphen** follow the $^1\text{O}_2$ pathway. However, **Rudppz** allows for supramolecular preorganization of NADH on the dppz ligand and thus enables an eT route. Under air, the

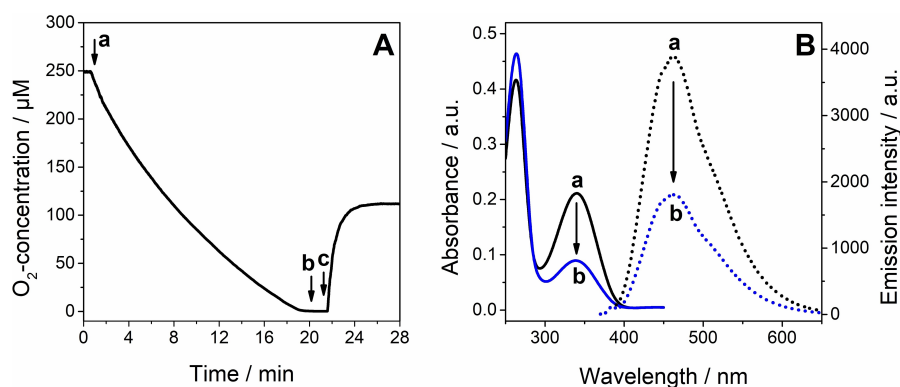
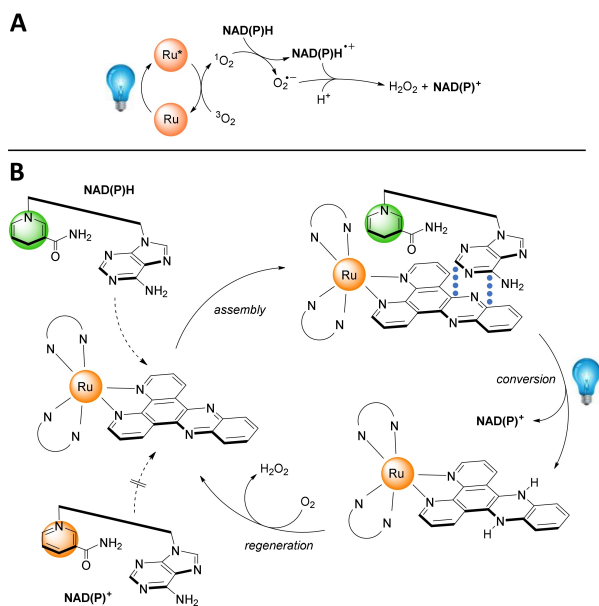


Figure 4. A) Course of O_2 -concentration during a typical NADH photooxidation experiment using a PBS buffered aqueous solution containing $500 \mu\text{M}$ NADH and $5 \mu\text{M}$ **Rudppz** under ambient conditions. Arrow a indicates the start of blue light irradiation of the solution which ends after ca. 20 min indicated by arrow b. Addition of catalase is marked by arrow c. B) UV-vis (solid lines) and corresponding emission spectra (dotted lines) of the reaction mixture before irradiation (black curves, a) and after complete consumption of oxygen (blue curves, b).



Scheme 2. Proposed photocatalytic mechanism for A) **Rutbbpy** and **Ruphen** as well as B) **Rudppz**.

catalytically inactive intermediate **Rudppz**_{H₂} gets finally reoxidized by oxygen to close the catalytic cycle.

To utilize the efficient eT pathway biochemically, we coupled the **Rudppz** mediated NAD(P)⁺ regeneration to an enzymatic model reaction. NADP-dependent malic enzyme (NADP-dependent oxaloacetate-decarboxylating malate dehydrogenase, EC 1.1.1.40, ME) was selected, converting L-malate into pyruvate in two steps. However, enzyme stability revealed to be the limiting factor of the envisaged photobiocatalytic process. In view of the reactivity of ¹O₂ towards various amino acids,^[42,43] irradiation (λ = 465 nm) of ME in presence of **Rutbbpy**, **Ruphen** and **Rudppz** led to the formation of inactive orange precipitates inhibiting further consumption of NADPH by **Rudppz** as well as NADP⁺ by ME. ¹O₂ formation by **Rudppz** most likely took place via binding into hydrophobic pockets of ME as evident from an increased and air sensitive luminescence of the complex in presence of the enzyme (Figure S51).^[21]

Therefore, a discontinuous protocol cycling between the different oxidation states of NADP was realized. First, photo-oxidation of NADPH was performed followed by ME addition in the dark. Both UV-vis absorption and emission spectroscopy clearly showed a successful cycling between NADPH and NADP⁺ proving the bioactivity of the generated oxidized nicotinamide (Figure 5). However, there are two possible explanations for the steadily decreasing efficiency of the photobiocatalytic process. Firstly, the formation of **Rudppz** containing precipitates during irradiation resulted in a lower amount of active complex in solution. Secondly, a potential co-presence of some non-precipitated enzyme continuously regenerated NADPH.

In conclusion, it was found that well-balanced supramolecular interactions can be utilized to overcome possible reactivity limitations of chromophores bearing short-lived excited states. By introducing a suitable cofactor binding site nearby a light-absorbing moiety, the preorganization induced mechanistic switch of NADH photooxidation from an ¹O₂ to an eT pathway allowed **Rudppz** to outperform Ru(II) prototype complexes, namely **Rutbbpy** and **Ruphen**. In future, the detailed insights into the catalytic mechanism gained in this study will allow further ligand-based optimization of visible light-driven NAD⁺ regeneration, finding application in photobiocatalysis and PDT. However, in view of the ¹O₂ sensitivity of different amino acids, technically optimized strategies such as permanent spatial separation^[44] of enzymes and ¹O₂ sensitizing chromophores will have to be pursued to guarantee continuous photobiocatalysis.

Acknowledgements

Supported by the Deutsche Forschungsgemeinschaft (DFG, German Research Foundation) – Projektnummern 364549901 – TRR 234 [A1] and 395358570. GMS acknowledges funding from the Novo Nordisk Fonden within the framework of the Fermentation Based Biomanufacturing education initiative (grant number NNF17SA0031362). Open Access funding enabled and organized by Projekt DEAL.

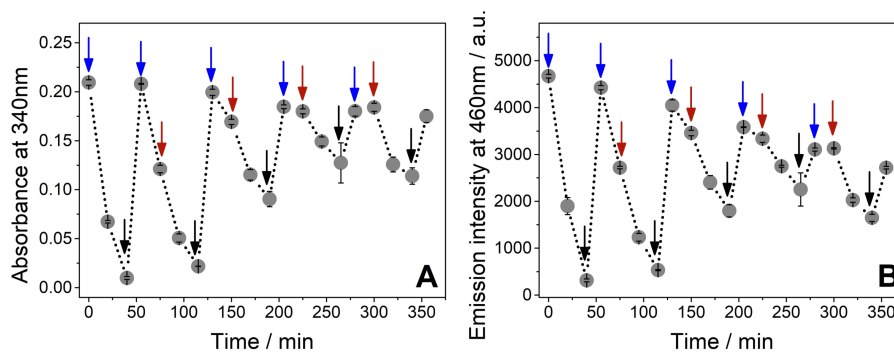


Figure 5. Discontinuous photobiocatalytic process followed by A) UV-vis absorption and B) emission spectroscopy. Arrows indicate the start of irradiation (blue), addition of ME after switching off the light source (black) and addition of fresh **Rudppz** after removal of the orange precipitates by centrifugation (red).

Conflict of Interest

The authors declare no conflict of interest.

Keywords: Cofactors · photooxidation · ruthenium · singlet oxygen · supramolecular chemistry

- [1] K. Robins, A. Osorio-Lozada, *Catal. Sci. Technol.* **2012**, *2*, 1524–1530.
- [2] W. Kroutil, H. Mang, K. Edegger, K. Faber, *Adv. Synth. Catal.* **2004**, *346*, 125–142.
- [3] L. G. Lee, G. M. Whitesides, *J. Am. Chem. Soc.* **1985**, *107*, 6999–7008.
- [4] H. K. Chenault, G. M. Whitesides, *Appl. Biochem. Biotechnol.* **1987**, *14*, 147–197.
- [5] C. Zhu, Q. Li, L. Pu, Z. Tan, K. Guo, H. Ying, P. Ouyang, *ACS Catal.* **2016**, *6*, 4989–4994.
- [6] G. Hilt, T. Jarbawi, W. R. Heineman, E. Steckhan, *Chem. Eur. J.* **1997**, *3*, 79–88.
- [7] S. Kochius, A. O. Magnusson, F. Hollmann, J. Schrader, D. Holtmann, *Appl. Microbiol. Biotechnol.* **2012**, *93*, 2251–2264.
- [8] S. Gargiulo, I. W. C. E. Arends, F. Hollmann, *ChemCatChem* **2011**, *3*, 338–342.
- [9] M. Rauch, S. Schmidt, I. W. C. E. Arends, K. Oppelt, S. Kara, F. Hollmann, *Green Chem.* **2017**, *19*, 376–379.
- [10] B. C. Ma, L. Caire da Silva, S.-M. Jo, F. R. Wurm, M. B. Bannwarth, K. A. I. Zhang, K. Sundmacher, K. Landfester, *ChemBioChem* **2019**, *20*, 2593–2596.
- [11] J. Handman, A. Harriman, G. Porter, *Nature* **1984**, *307*, 534–535.
- [12] R. Maidan, I. Willner, *J. Am. Chem. Soc.* **1986**, *108*, 1080–1082.
- [13] R. Ruppert, E. Steckhan, *J. Chem. Soc. Perkin Trans. 2* **1989**, 811–814.
- [14] C. Ge, J. Zhu, A. Ouyang, N. Lu, Y. Wang, Q. Zhang, P. Zhang, *Inorg. Chem. Front.* **2020**, *7*, 4020–4027.
- [15] H. Huang, S. Banerjee, K. Qiu, P. Zhang, O. Blacque, T. Malcomson, M. J. Paterson, G. J. Clarkson, M. Staniforth, V. G. Stavros, et al., *Nat. Chem.* **2019**, *11*, 1041–1048.
- [16] C. Huang, C. Liang, T. Sadhukhan, S. Banerjee, Z. Fan, T. Li, Z. Zhu, P. Zhang, K. Raghavachari, H. Huang, *Angew. Chem. Int. Ed.* **2021**, *60*, 9474–9479; *Angew. Chem.* **2021**, *133*, 9560–9565.
- [17] F. Petrat, S. Pindiur, M. Kirsch, H. De Groot, *J. Biol. Chem.* **2003**, *278*, 3298–3307.
- [18] G. Peters, M. A. J. Rodgers, *Biochim. Biophys. Acta* **1981**, *637*, 43–52.
- [19] R. L. Willson, *J. Chem. Soc. D* **1970**, 1005.
- [20] E. J. Land, A. J. Swallow, *Biochim. Biophys. Acta* **1971**, *234*, 34–42.
- [21] A. E. Friedman, J.-C. Chambron, J.-P. Sauvage, N. J. Turro, J. K. Barton, *J. Am. Chem. Soc.* **1990**, *112*, 4960–4962.
- [22] C. Moucheron, A. Kirsch-De Mesmaeker, S. Choua, *Inorg. Chem.* **1997**, *36*, 584–592.
- [23] H. Niyazi, J. P. Hall, K. O'Sullivan, G. Winter, T. Sorensen, J. M. Kelly, C. J. Cardin, *Nat. Chem.* **2012**, *4*, 621–628.
- [24] H. Song, J. T. Kaiser, J. K. Barton, *Nat. Chem.* **2012**, *4*, 615–620.
- [25] S. Rau, B. Schäfer, A. Grüßing, S. Schebesta, K. Lamm, J. Vieth, H. Görls, D. Walther, M. Rudolph, U. W. Grummt, et al., *Inorg. Chim. Acta* **2004**, *357*, 4496–4503.
- [26] J. De Ruyck, M. Famerée, J. Wouters, E. A. Perpète, J. Preat, D. Jacquemin, *Chem. Phys. Lett.* **2007**, *450*, 119–122.
- [27] T. Saba, J. W. H. Burnett, J. Li, P. N. Kechagiopoulos, X. Wang, *Chem. Commun.* **2020**, *56*, 1231–1234.
- [28] C. Mari, V. Pierroz, R. Rubbiani, M. Patra, J. Hess, B. Spingler, L. Oehninger, J. Schur, I. Ott, L. Salassa, et al., *Chem. Eur. J.* **2014**, *20*, 14421–14436.
- [29] R. Bodaness, P. Chan, *J. Biol. Chem.* **1977**, *252*, 8554–8560.
- [30] M. Y. Li, C. S. Cline, E. B. Koker, H. H. Carmichael, C. F. Chignell, P. Bilski, *Photochem. Photobiol.* **2001**, *74*, 760.
- [31] J. Méndez-Hurtado, R. López, D. Suárez, M. I. Menéndez, *Chem. Eur. J.* **2012**, *18*, 8437–8447.
- [32] R. Nilsson, D. R. Kearns, B. Paul, R. Kearns, *J. Am. Chem. Soc.* **1972**, *94*, 1030–1031.
- [33] D. A. McGovern, A. Selmi, J. E. O'Brien, J. M. Kelly, C. Long, *Chem. Commun.* **2005**, 1402–1404.
- [34] B. Czochralska, L. Lindqvist, *Chem. Phys. Lett.* **1983**, *101*, 297–299.
- [35] S. Fukuzumi, O. Inada, T. Suenobu, *J. Am. Chem. Soc.* **2003**, *125*, 4808–4816.
- [36] J. Gébicki, A. Marcinek, J. Zielonka, *Acc. Chem. Res.* **2004**, *37*, 379–386.
- [37] E. J. C. Olson, D. Hu, A. Hörmann, A. M. Jonkman, M. R. Arkin, E. D. A. Stemp, J. K. Barton, P. F. Barbara, *J. Am. Chem. Soc.* **1997**, *119*, 11458–11467.
- [38] C. R. Martinez, B. L. Iverson, *Chem. Sci.* **2012**, *3*, 2191–2201.
- [39] F. L. Huber, S. Amthor, B. Schwarz, B. Mizaikoff, C. Streb, S. Rau, *Sustain. Energy Fuels* **2018**, *2*, 1974–1978.
- [40] C. E. Paul, E. Churakova, E. Maurits, M. Girhard, V. B. Urlacher, F. Hollmann, *Bioorg. Med. Chem.* **2014**, *22*, 5692–5696.
- [41] K. Kobayashi, H. Ohtsu, K. Nozaki, S. Kitagawa, K. Tanaka, *Inorg. Chem.* **2016**, *55*, 2076–2084.
- [42] R. S. Bodaness, *Biochem. Biophys. Res. Commun.* **1982**, *108*, 1709–1715.
- [43] M. J. Davies, *Photochem. Photobiol. Sci.* **2004**, *3*, 17–25.
- [44] J. S. Lee, S. H. Lee, J. H. Kim, C. B. Park, *Lab Chip* **2011**, *11*, 2309–2311.

Manuscript received: August 18, 2021

Accepted manuscript online: September 21, 2021

Version of record online: October 21, 2021